

Precise fission fragment anisotropies for the $^{12}\text{C} + ^{232}\text{Th}$ reaction: Supporting the nuclear orientation dependence of quasifission

J. C. Mein, D. J. Hinde, M. Dasgupta, J. R. Leigh, J. O. Newton, and H. Timmers
Department of Nuclear Physics, Research School of Physical Sciences and Engineering,

Australian National University, Canberra, ACT 0200, Australia

(Received 25 September 1996)

Recently measured fission fragment angular anisotropies for the reaction $^{12}\text{C} + ^{232}\text{Th}$ show unusual behavior compared to other reactions of ^{12}C , ^{16}O , and ^{19}F on actinide targets at energies below the fusion barrier. As a result, doubts have been raised about the hypothesis that large sub-barrier anisotropies are due to the occurrence of quasifission when the projectiles collide with the tips of the deformed actinide target nuclei. To investigate this inconsistency, fission fragment angular distributions for this reaction were measured to high precision in the bombarding energy range 57–75 MeV. Fission following transfer reactions was identified and rejected at all angles using the deduced velocity vector of the fissioning nuclei. Cross sections and anisotropies for full momentum transfer fission were determined, and the fusion barrier distribution was extracted. These data support the interpretation that the dependence of the competition between quasifission and fusion fission on the orientation of the deformed actinide nucleus can explain the large sub-barrier anisotropies. [S0556-2813(97)50403-1]

PACS number(s): 25.70.Jj

Measured angular distributions for fission following heavy-ion bombardment of heavy targets exhibit larger anisotropies [1] than predicted by the transition state model (TSM) [2]. This has been attributed to the quasifission mechanism, where an elongated nucleus (dinucleus) is assumed to be formed, rather than a compact compound nucleus. The dinucleus evolves over the potential energy surface, approaching mass equilibrium, then undergoes scission [1,3].

With decreasing bombarding energies, the anisotropies generally decrease. However, it was observed that for reactions with actinide targets at near-barrier energies, the anisotropies were not only much larger than TSM predictions, but increased [4–10] as the beam energy dropped through the fusion barrier region. This anomalous behavior has been observed clearly in the reactions of ^{12}C , ^{16}O , and ^{19}F with ^{232}Th and ^{238}U , in particular.

A number of explanations for this anomalous behavior have been proposed. Assuming that a compact configuration is formed, it has been proposed that the TSM fails for such fissile systems, and that fission occurs before equilibration of one or more degrees of freedom. This has been called pre-equilibrium fission [11–13].

The observed correlation between the anisotropies and the fusion barrier distribution for the reaction $^{16}\text{O} + ^{238}\text{U}$ led to a different interpretation of the anomalous anisotropies [6,10]. It was proposed that quasifission is in competition with fusion fission, the probability depending on the orientation of the deformed target nucleus [6] with respect to the projectile at the time of the collision. This hypothesis was supported by the increasing asymmetry observed [10] in the fission mass distributions as the bombarding energy decreased through the fusion barrier region.

Fission anisotropies for the reaction $^{12}\text{C} + ^{232}\text{Th}$ have recently been measured at sub-barrier energies by Majumdar *et al.* [9]. Their data show an abrupt rise in anisotropy, to a

value of ~ 2.1 , as the bombarding energy decreases through the fusion barrier region, followed by a rapid decline, producing a high narrow peak centered at $E_{\text{c.m.}} \approx 59$ MeV. These data are consistent with the previous measurement of Ref. [8], performed at the same laboratory. It was claimed in Ref. [9] that the quasifission model of Ref. [6] cannot explain these data in a consistent way. This unexpected result throws doubt on the quasifission interpretation, or at least may be evidence for a new feature in fission anisotropies.

In contrast, a more recent measurement by Lestone *et al.* [14] found no peak. Instead the anisotropies maintain a near-constant value of 1.5 in the region of the fusion barrier. The serious conflict between the two data sets consistent with a peak, and the single data set consistent with a plateau, necessitated a further measurement to resolve this disagreement, and clarify the physical processes occurring in sub-barrier fission reactions.

The experimental techniques available to us allowed the reduction or elimination of many possible sources of uncertainty in the measured anisotropies. All angles in the angular distributions were measured simultaneously. Using pulsed beams, the data could be analyzed using a technique which allows separation and rejection of transfer fission events at all angles, using the deduced velocity vector of each fissioning nucleus. This also allows the identification of fission resulting from lighter target contaminants; none was observed. Small statistical uncertainties were obtained, while systematic errors were checked using a ^{252}Cf source. Measurement at regular energy intervals allowed determination of the fusion barrier distribution, which could indicate any possible unusual behavior in this reaction.

The experiment was performed using the 14UD tandem electrostatic accelerator at the Australian National University. Pulsed beams of ^{12}C (1 ns bursts separated by 106 ns) were incident on a target of ^{232}Th of $\approx 80 \mu\text{g cm}^{-2}$ thickness, deposited on a $\approx 30 \mu\text{g cm}^{-2}$ carbon foil. Beam ener-

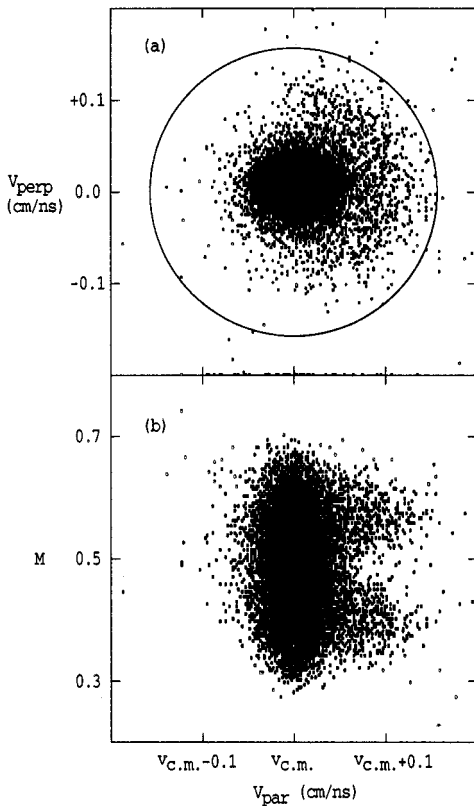


FIG. 1. (a) The deduced velocity components of the fissioning nuclei, for the reaction $^{12}\text{C}+^{232}\text{Th}$ at $E_{\text{lab}}=67$ MeV, for $\theta_{\text{lab}}=100^\circ$. (b) v_{par} against mass-split M , showing clearly the transfer fission events, with large values of v_{par} , and an asymmetric mass-split M (see text).

gies E_{lab} were varied from 57 to 75 MeV, in 2 MeV steps. Coincident fission fragments were measured using two large area multiwire proportional counters (MWPC) of the CUBE detector array, giving scattering angle coverages of $-171^\circ < \theta_{\text{lab}} < -94^\circ$ and $4^\circ < \theta_{\text{lab}} < 81^\circ$ with respect to the beam. The target was located in the center of the CUBE, and two monitor detectors were placed at $\pm 23^\circ$, above and below the beam axis, to enable the determination of absolute cross sections.

The MWPC detectors were position sensitive in two dimensions, and each event at position (x,y) was transformed to give the scattering angle θ_{lab} and the azimuthal angle ϕ with respect to the beam axis, for both fragments. The velocities of each fragment were also determined, allowing reconstruction of the kinematics of each event.

Fission of the target-like nuclei following transfer reactions (transfer fission) must be separated from full-momentum transfer (FMT) fission, in which the projectile amalgamates completely with the target. This was accomplished using the deduced velocity vector technique, details of which are given in Ref. [10]. Figure 1(a) shows an example of the distribution of the deduced velocity component of the fissioning nuclei parallel to the beam (v_{par}) against the component perpendicular both to the beam and the scission axis (v_{perp}). FMT fission events are tightly grouped in the center of the plot, while transfer fission events scatter within the kinematic limit indicated by the circle. Figure 1(b) shows

the deduced fission mass-split M against v_{par} . The transfer fission events stand out clearly, having an asymmetric mass split, and at this energy, a larger v_{par} than FMT fission, due to the projectilelike nucleus recoiling to backward angles. As in Ref. [10], FMT fission events were selected by firstly accepting only the central region in v_{par} around $v_{\text{c.m.}}$, then projecting the distribution of v_{perp} and fitting the FMT peak and a flat (transfer fission) background. This reaction showed lower proportions of transfer fission than the $^{16}\text{O}+^{238}\text{U}$ reaction [10], with typically less than $\approx 5\%$ of all fission resulting from transfer fission.

The angular distributions in the back detector were obtained for 5° cuts in θ_{lab} . These were transformed into the center-of-mass reference frame using the Viola systematics [15] for symmetric fission. The anisotropies were determined from the fits to the angular distributions using the procedure of Refs. [1,16], and are defined as the ratio of the yield at 180° to that at 90° , denoted by $W(180^\circ)/W(90^\circ)$. The possible presence of systematic errors was investigated by determining the anisotropy for two ^{252}Cf source measurements, which gave a value of 1.034 ± 0.011 . This shows that the systematic error in the extracted anisotropies is not significant. The large number of fission events collected at each energy ($\approx 5 \times 10^4$ at $E_{\text{c.m.}}=56$ MeV, and $\geq 10^5$ at higher energies) resulted in low statistical uncertainties in the angular distributions.

The fission anisotropies deduced from the angular distributions are shown in Fig. 2(a). Those for all fission events are shown by hollow circles, while those for FMT fission are denoted by filled circles. Because of the small proportion of transfer fission, the two data sets are not very different. The FMT anisotropies exhibit a broad, low peak centered at an energy close to the mean fusion barrier height, with a maximum anisotropy of 1.53 ± 0.03 .

The fusion cross sections σ_{fus} were extracted from the integration of the angular distributions for FMT fission. The fusion barrier distribution [17] was determined from the second derivative of the function $E_{\text{c.m.}}\sigma_{\text{fus}}$ with respect to $E_{\text{c.m.}}$, using a point-difference formula [18] with an energy step of 1.90 MeV, and is shown in Fig. 2(b). It displays the wide asymmetric shape expected for a deformed prolate nucleus with a positive hexadecapole moment [6,18].

The standard model for the interpretation of fission fragment angular distributions, following fusion fission, is the transition state model (TSM). The model requires knowledge of three quantities: the effective moment of inertia at the saddle-point deformation, and the distribution of angular momentum and temperature at the saddle point. The effective moment of inertia at the saddle point was obtained from a simple parametrization [19] of the rotating finite range model (RFRM) [20]. The angular momentum distributions of the fissioning nuclei were calculated with the approximate coupled channels code CCMOD [21], using the established deformation parameters for ^{232}Th . The calculated fusion barrier distribution reproduces reasonably well the measured data, as is shown in Fig. 2(b).

The distribution of temperatures of the fissioning nuclei at the saddle point for a given bombarding energy was determined from the Monte Carlo code JOANNE [22], constrained by precission neutron multiplicities ν_{pre} , which were measured at three energies in Ref. [23] for the $^{12}\text{C}+^{232}\text{Th}$ reac-

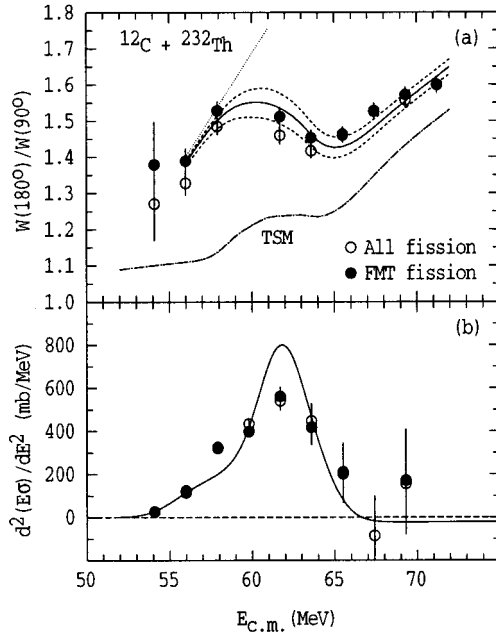


FIG. 2. (a) Fission anisotropies for the $^{12}\text{C} + ^{232}\text{Th}$ reaction. The open circles represent the case where no discrimination against transfer fission is made. The filled circles represent the anisotropies for FMT fission only. The expected anisotropy based on the transition state model is given by the dot-dashed line. The solid and dashed lines show the results of the quasifission model described in the text. (b) The second derivative with respect to energy of the fusion excitation function, multiplied by $E_{c.m.}$, which is proportional to the fusion barrier distribution. The solid line shows the barrier distribution calculated assuming a permanent deformation for the target nuclei.

tion. The presaddle delay time τ_{pre} and the saddle-to-scission delay time τ_{ssc} were adjusted until the three ν_{pre} data points were fitted. The delay times adopted were $\tau_{pre}=10$ zs and $\tau_{ssc}=20$ zs, which are consistent with the precission, or transient, delay time as well as the total dynamical delay time of Ref. [23].

From the inputs described above, TSM calculations of the anisotropies were performed following the procedure detailed in Ref. [16]. The results are shown in Fig. 2(a) by the dot-dashed line. They deviate from the experimental data at all energies, in a similar manner to that observed for the $^{16}\text{O} + ^{238}\text{U}$ reaction [6,10].

This disagreement can be resolved using the model of Ref. [6], where it was assumed that collisions with the tips of deformed actinide nuclei lead to quasifission, while collisions with the sides result in fusion fission. For simplicity a sharp transition between quasi-fission and fusion fission was assumed to occur at a critical fusion radius, which corresponded to a critical angle θ_{cr} between the beam axis and the symmetry axis of the target nucleus. This model was applied to the $^{12}\text{C} + ^{232}\text{Th}$ FMT fission anisotropies and the resulting calculation is shown in Fig. 2(a). The anisotropy for quasifission was assumed to increase with beam energy, in a way consistent with the anisotropies at the lowest energies (dotted line). The assumption of an increasing angular anisotropy with beam energy for quasifission is reasonable, based on the observation of rapidly increasing anisotropies for reactions where quasifission is dominant [1,24].

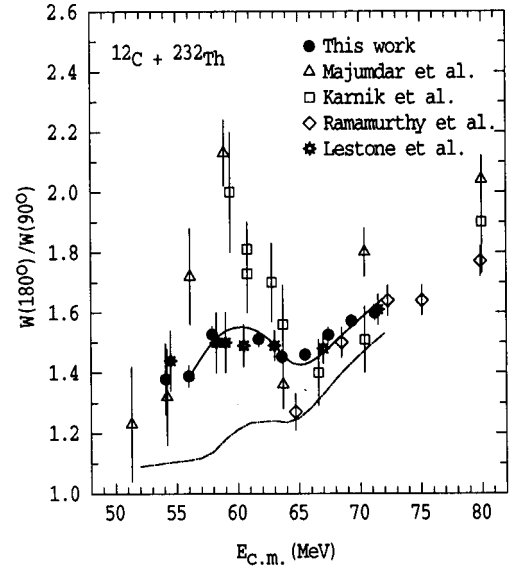


FIG. 3. The fission anisotropies for the $^{12}\text{C} + ^{232}\text{Th}$ reaction showing the FMT fission from this work (solid circles), compared to previously measured anisotropies from Ref. [8] (squares), Ref. [9] (triangles), Ref. [12] (diamonds), and Ref. [14] (stars), adapted from figures in those references.

The best reproduction of the experimental anisotropies was achieved with a critical angle of $\theta_{cr}=18^\circ$ (solid line). The effect of a range of $\pm 2^\circ$ is also shown in Fig. 2(a) by the short dashed lines. This critical angle is consistent with those reported by Majumdar *et al.* [9] for the reactions ^{16}O and $^{19}\text{F} + ^{232}\text{Th}$.

Figure 3 compares all the experimental anisotropy data available for the $^{12}\text{C} + ^{232}\text{Th}$ reaction. Our FMT fission anisotropies measured at energies above the fusion barrier region are consistent with the previous measurements [8,9,12,14] shown in the figure. In the region of the barrier it is clear that the data are divided into two groups, those of Ref. [8,9], which show a peak anisotropy of ~ 2.1 at $E_{c.m.} \approx 59$ MeV, and those reported here, and in Ref. [14] showing a peak value of ~ 1.5 . The anisotropies all agree again at the lowest energies measured.

The precautions taken in our experimental measurement and analysis to eliminate the contribution from transfer fission do not make a large difference to the anisotropies, because of the low proportions of transfer fission. Our data thus agree well with the results of Lestone *et al.*, where transfer fission was not discriminated against. It would be interesting to compare the anisotropies measured by Majumdar *et al.* before and after subtraction of the transfer fission component, to confirm that their technique also results in a small correction. Unless the transfer fission component had in error been oversubtracted, it is very difficult to explain the discrepancy between the data presented by Majumdar *et al.*, and the lower anisotropies determined both in this work, and in Ref. [14].

The results of the measurement presented here are consistent with the measured trends in anisotropies for other reactions on actinide targets. They support the interpretation that the anomalously large fission anisotropies observed at sub-barrier energies arise from the occurrence of quasifission when the projectiles interact with the tips of the deformed actinide target nuclei.

- [1] B.B. Back, R.R. Betts, J.E. Gindler, B.D. Wilkins, S. Saini, M.B. Tsang, C.K. Gelbke, W.G. Lynch, M.A. McMahan, and P.A. Baisden, *Phys. Rev. C* **32**, 195 (1985).
- [2] R. Vandenbosch and J.R. Huizenga, *Nuclear Fission* (Academic Press, New York, 1973).
- [3] J. Töke, R. Bock, G.X. Dai, A. Gobbi, S. Gralla, K.D. Hildenbrand, J. Kuzminski, W.J.F. Müller, A. Olmi, and H. Stelzer, *Nucl. Phys.* **A440**, 327 (1985).
- [4] T. Murakami, C.-C. Sahm, R. Vandenbosch, D.D. Leach, A. Ray, and M.J. Murphy, *Phys. Rev. C* **34**, 1353 (1986).
- [5] H. Zhang, Z. Liu, J. Xu, X. Quian, Y. Qiao, C. Lin, and K. Xu, *Phys. Rev. C* **49**, 926 (1994), and references therein.
- [6] D.J. Hinde, M. Dasgupta, J.R. Leigh, J.P. Lestone, J.C. Mein, C.R. Morton, J.O. Newton, and H. Timmers, *Phys. Rev. Lett.* **74**, 1295 (1995).
- [7] N. Majumdar, P. Bhattacharya, D.C. Biswas, R.K. Choudhury, D.M. Nadkarni, and A. Saxena, *Phys. Rev. C* **51**, 109 (1995).
- [8] A. Karnik, S. Kailas, A. Chatterjee, P. Singh, A. Navin, D.C. Biswas, D.M. Nadkarni, A. Shrivastava, and S.S. Kapoor, *Z. Phys. A* **351**, 195 (1995).
- [9] N. Majumdar, P. Bhattacharya, D.C. Biswas, R.K. Choudhury, D.M. Nadkarni, and A. Saxena, *Phys. Rev. C* **53**, R544 (1996).
- [10] D.J. Hinde, M. Dasgupta, J.R. Leigh, J.C. Mein, C.R. Morton, J.O. Newton, and H. Timmers, *Phys. Rev. C* **53**, 1290 (1996).
- [11] V.S. Ramamurthy and S.S. Kapoor, *Phys. Rev. Lett.* **54**, 178 (1985).
- [12] V.S. Ramamurthy, S.S. Kapoor, R.K. Choudhury, A. Saxena, D.M. Nadkarni, A.K. Mohanty, B.K. Nayak, S.V. Sastry, S. Kailas, A. Chatterjee, P. Singh, and A. Navin, *Phys. Rev. Lett.* **65**, 25 (1990).
- [13] Z. Liu, H. Zhang, J. Xu, Y. Qiao, Z. Qian, and C. Lin, *Phys. Lett. B* **353**, 173 (1995).
- [14] J.P. Lestone, A.A. Sonzogni, M.P. Kelly, and D. Prindle, *Phys. Rev. C* **55**, R16 (1997).
- [15] V.E. Viola, K. Kwiatkowski, and M. Walker, *Phys. Rev. C* **31**, 1550 (1985).
- [16] C.R. Morton, D.J. Hinde, J.R. Leigh, J.P. Lestone, M. Dasgupta, J.C. Mein, J.O. Newton, and H. Timmers, *Phys. Rev. C* **52**, 243 (1995).
- [17] N. Rowley, G.R. Satchler, and P.H. Stelson, *Phys. Lett. B* **254**, 25 (1991).
- [18] J.X. Wei, J.R. Leigh, D.J. Hinde, J.O. Newton, R.C. Lemmon, S. Elfström, and J.X. Chen, *Phys. Rev. Lett.* **67**, 3368 (1991).
- [19] J.P. Lestone, *Phys. Rev. C* **51**, 580 (1995).
- [20] A.J. Sierk, *Phys. Rev. C* **33**, 2039 (1986).
- [21] M. Dasgupta, A. Navin, Y.K. Agarwal, C.V.K. Baba, H.C. Jain, M.L. Jhingan, and A. Roy, *Nucl. Phys.* **A539**, 351 (1992).
- [22] J.P. Lestone, J.R. Leigh, J.O. Newton, D.J. Hinde, J.X. Wei, J.X. Chen, S. Elfström, and M. Zielinska-Pfabé, *Nucl. Phys.* **A559**, 288 (1989).
- [23] A. Saxena, A. Chatterjee, R.K. Choudhury, S.S. Kapoor, and D.M. Nadkarni, *Phys. Rev. C* **49** 932, (1994).
- [24] D.J. Hinde, C.R. Morton, M. Dasgupta, J.R. Leigh, J.C. Mein, and H. Timmers, *Nucl. Phys.* **A592**, 271 (1995).